

Effect of Upstream Velocity Gradient on the Formation of Sink Vortices in a Jet Engine Test Cell

W. H. Ho, H. Dumbleton, and M.C. Jermy

Abstract— Vortices can be produced and ingested into the intake of a jet engine during high power operation in the vicinity of solid surfaces causing Foreign Object Damage (FOD) or compressor stall and engine surge problems. This can occur when the engine is mounted on the wing of a plane during take-off and engine ground runs or when the engine is placed inside a test cell for testing after an engine overhaul and prior to reinstallation onto the aircraft.

Procedures have been put in place to prevent such damage from occurring on the runway. However to prevent such vortices from forming, especially in the test cells, it is necessary to be able to predict the onset of the vortex or at least to understand the factors affecting the formation of such vortices.

Vortex formation in an enclosed cell is different from vortex formation over a solid plane (runway scenario). Ho and Jermy investigated vortex formation using a suction tube in a open-end box model simulating an engine in a test cell scenario and found that 3 distinct regimes of flow (regular vortex, deformed vortex and no vortex) exists as opposed to the simple vortex/no vortex flow for runway scenario.

This paper extends the work by first investigating the effects changing upstream velocity gradient has on the threshold and then investigating the potential source of this upstream velocity gradient in real cells using two separate CFD simulations.

The results show that an increase in upstream velocity gradient (s) increases the range of conditions over which a vortex forms. All three regimes show signs of shifting the threshold of vortex formation to lower ratio of inlet velocity over upstream average velocity (V_i/V_o) for a given ratio of inlet height over inlet diameter (H/D_i).

A separate set of simulations performed showed that wind blowing across the intake stack of a U-shaped jet engine test cell produces net vorticity in the upstream plane perpendicular to the longitudinal direction of the of the suction tube. This vorticity is implicated in the formation of the vortices.

Index Terms— CFD, Fluent, Vortex.

I. INTRODUCTION

Vortices can develop in the intakes of aero engines during

Manuscript received January 8, 2008.

W.H. Ho is with the Department of Mechanical Engineering, University of Canterbury, Christchurch, New Zealand (phone: 643-364-2987 x7866; fax: 643-364-2078; e-mail: whh19@student.canterbury.ac.nz).

H. Dumbleton, was with the Department of Mechanical Engineering, University of Canterbury, Christchurch, New Zealand. He has now graduated.

M.C. Jermy is with the Department of Mechanical Engineering, University of Canterbury, Christchurch, New Zealand (e-mail: mark.jermy@canterbury.ac.nz).

high power operation near solid surfaces. This may occur during take-off or during test in a ground facility. The structure of the vortex is similar to the vortex seen in a bath. One end of the vortex is anchored on the nearby solid surface while the other enters the suction intake.

In a test cell, vortices if present are seen to be anchored to the ceiling of the cell. Ho and Jermy [i] showed that a low velocity region present near one of the horizontal surfaces would force the vortex to attach to that surface. This low velocity region is likely to be present near the ceiling of the main test chamber in a U-shaped test cell and is seen in CFD simulation of U-shaped real cells. The vortex where present is known to attach to the ceiling.

In a test cell, there is a flow of excess air beyond that required by the engine, driven by entrainment by the exhaust jet plume. This flow passes between the engine and the internal walls of the cell. It is quantified by a cell bypass ratio (CBR):

$$CBR = 100\% \left(\frac{\dot{m}_{cell} - \dot{m}_{engine}}{\dot{m}_{engine}} \right)$$

Where \dot{m}_{cell} is the air mass flow rate at the cell intake and \dot{m}_{engine} is the air mass flow rate through the engine including the fan and core. The CBR is distinct from the engine bypass ratio, which is the ratio of the fan to core flow rate.

A commonly used rule of thumb is that a cell must have a bypass ratio of more than 80% to avoid vortex formation. Typically cells are designed with CBRs up to, and in some cases exceeding, 200%.

CFD simulations of intake vortices have been reported by [ii], [iii] and Ho and Jermy [i] have used CFD simulations to show the different flow regimes present in a test cell like scenario. However, no studies to date have shown the effects of different flow and geometry parameters have on the vortex formation threshold.

The upstream velocity gradient has been shown experimentally and numerically to have a positive correlation with probability of vortex formation [iv], [v] on a runway like scenario and it is anticipated to have the similar effects in the test cell.

II. VORTEX FORMATION

The vortex type concerned in both these studies is the type which concentrates ambient vorticity leading to a vortex with a single core. This study does not consider the types which do

not require ambient vorticity and which manifest vortex systems with two or more cores.

In the formation of such vortices, there exists a blow-away velocity. The blow-away velocity is the threshold velocity of upstream air above which the vortex core is convected downstream and disconnected from the inlet. Conversely if the upstream air velocity is below the blow-away velocity a vortex may be formed, subject to other conditions being favourable.

Similar to previous studies, the blow away condition is expressed as the ratio of the inlet velocity V_i to the freestream velocity V_o . There is a minimum value of this ratio V_i/V_o below which the vortex will not form.

On the other hand, if the inlet is too far away from a solid surface, there will be no stagnation point [vi] (a point with a diverging velocity profile radially) on the surface and the vortex cannot form. In other words, the capture stream-tube (enclosing the air which enters the inlet) does not intersect with any solid surface. This condition is expressed as the ratio of the perpendicular distance from the inlet to the solid surface H to the inlet internal diameter D_i . There is a maximum value of this ratio H/D_i above which the vortex will not form.

The threshold values of these two ratios are interdependent and can be expressed as lines differentiating the different regions on a V_i/V_o versus H/D_i graph indicating the different flow regimes as shown in Figure 1.

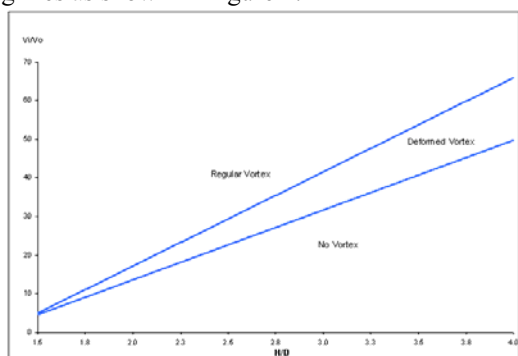


Figure 1: Different flow regimes present in the test cell like model simulations

III. VORTEX FORMATION IN TEST CELL LIKE STRUCTURE

Previous studies have shown that whilst there exists only two distinct flow regimes (vortex formed or no vortex formed) when a suction tube is placed over a solid surface, another flow regime develops when walls are placed over the tube. This additional flow regime was demonstrated by Ho and Jermy [i]. The flow regime was named deformed vortex and is characterised by vortex core being irregular in shape, the location of the vortex not being directly below the suction inlet and the unsteady nature of the vortex core.

The parameters that are likely to affect the threshold of each of the regimes include the following:

1. The distance between the walls and the engine
2. The size of the engine inlet
3. The distance between the cell inlet and the engine inlet
4. The cell inlet velocity gradient
5. The cell inlet velocity
6. The engine inlet flow velocity or flow rate

This paper addresses point 4.

IV. METHOD

The simulations will be conducted on the same model as those used by Ho and Jermy [i] using ANSYS Fluent. The geometry was meshed with Gambit 2.2.30 with tetrahedral/hybrid meshes throughout. A typical mesh is shown in Figure 2 below.

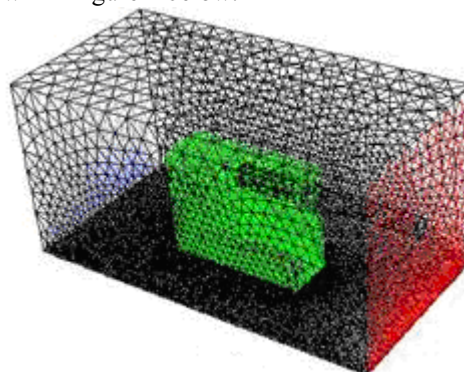


Figure 2: Effect of upstream velocity gradient simulation CFD mesh. The central region has a tighter mesh compared to the rest of the cell as this is where the vortex appears.

The eventual mesh has between 100 000 to 200 000 cells.

The boundary conditions for the model are as follows:

- Cell Inlet – Velocity Inlet UDF defining a linear velocity profile with a low velocity region near one of the surfaces.
- Engine Inlet - Outflow with Flow Rate Rating of 1
- Cell Outlet – Outflow with Flow Rate Rating set to achieve the desired Cell Bypass Ratio
- Cell and Engine Walls – No-slip walls (zero velocity on the surface)
- The solution was initialised from the Cell Inlet plane.

A. Compressible vs. Incompressible Flow

Incompressible flow solver was used as accordance to Ho and Jermy [i].

B. Turbulence Model

Turbulence was modelled with the SST $k-\omega$ scheme. This scheme was chosen as combining the best features of the $k-\epsilon$ scheme in free flows and the standard $k-\omega$ scheme in near wall flows, yet avoiding the computational expense of the Reynolds stress models. The difference in the two models has been investigated by Jermy and Ho [iv] and the SST- $k\omega$ turbulence model produced similar results to the RSM model.

C. Mesh Convergence

A mesh convergence test was conducted and the eventual mesh (after mesh independence was achieved) used had a mesh size as follows (the description are those as used in Gambit):

- Ground (Green Zone) – 0.1m Quad
- Ground (Rest of Cell) – 0.2m Tri
- Cell (Green Region) – 0.35 – 0.5m Tetrahedral
- Cell (Rest of Cell) – 1m Tetrahedral
- Where the suction inlet diameter takes a value of 1m

D. Upstream Velocity Gradients

Three different upstream velocity gradients were solved and they are 0.2/s, 0.3/s and 0.4/s. The upstream average

velocity was kept at a constant value to negate the effects of different Reynolds number which has been found to affect the vortex formation threshold in the runway scenarios and could be the same in the test cell scenario.

V. RESULTS

The solution schemes used were as follows:

- Pressure Based Solver
- First Order Discretisation scheme

The solution was initialised from cell inlet at the start of every solution to prevent a numerical equivalent of the “hysteresis effect” in which the location of the vortex formation threshold depends on whether the inlet velocity or inlet suction separation distance is increased or decreased, observed by Ridder and Samuelsson [vii] in their experiments.

All other solver settings were left as default values.

A. Stages of Vortex Formation

All 3 stages of flow regime was observed in the simulations and the illustration of all three regimes are shown in Figure 3 (vector plot) and Figure 4 (pathline plot) below

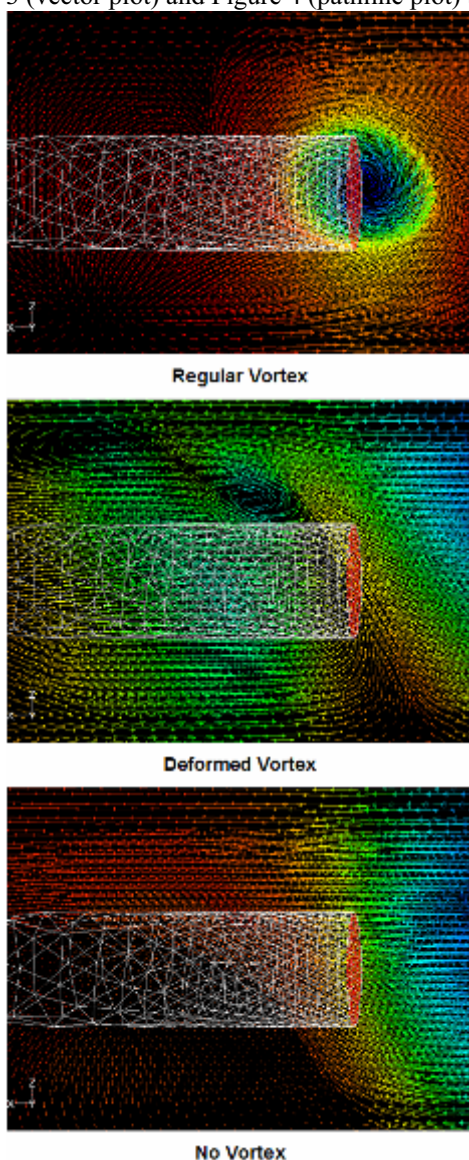


Figure 3: Vector plot illustrations for the three flow regimes

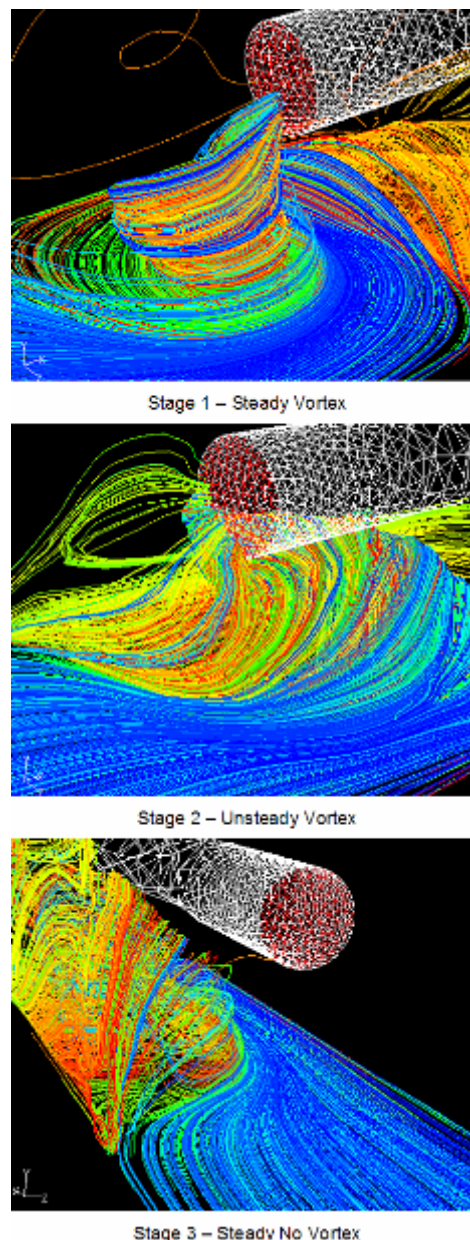


Figure 4: Pathline illustrations of the three flow regimes

B. Vortex Formation Threshold

The vortex formation threshold is defined as the value of V_i/V_o (ratio of the average velocity at the engine inlet to the average velocity at the cell inlet) at which each flow regime starts and ends.

The model was solved with cell bypass ratio increasing in steps of 5% until the threshold for the three stages are found. This translates into an uncertainty in V_i/V_o of not more than $\pm 2.6\%$.

The vortex formation threshold with a 0.2/s upstream average velocity gradient is shown in Figure 5 below. The values for the other velocity gradients are similar to these.

The vortex formation threshold with varying cell inlet velocity gradient is shown in Figure 6 below with the solid line showing the boundary between the steady and deformed vortex regime and the dotted line showing the boundary between the deformed and no vortex regime.

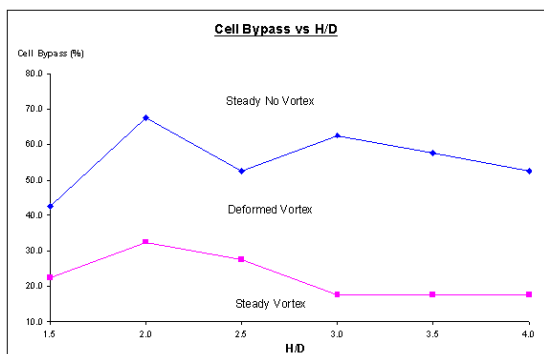


Figure 5: Vortex formation threshold for upstream velocity gradient = 0.2 in terms of CBR.

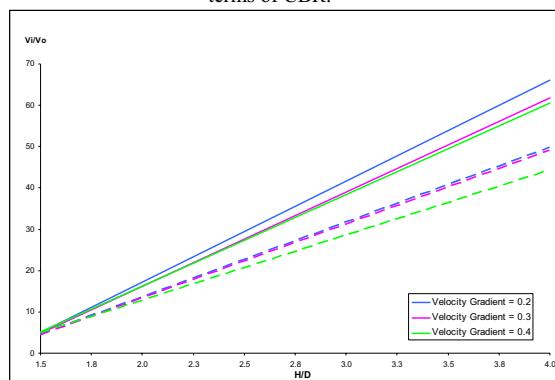


Figure 6: Vortex formation threshold for various upstream velocity gradient in terms of V_i/V_o

C. Effects of cross-wind

A separate CFD simulation was conducted using Fluent to investigate how the direction of the wind blowing around the intake stack of a U-shaped test cell affects the upstream velocity gradient. A CFD model was created of a vertical intake stack, turning vanes and the front portions of the main engine chamber. The CFD model and mesh is shown in Figure 7 and Figure 8 respectively.

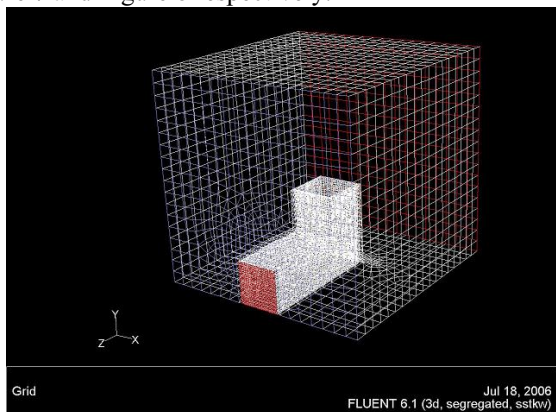


Figure 7: Effect of cross-wind simulation CFD model

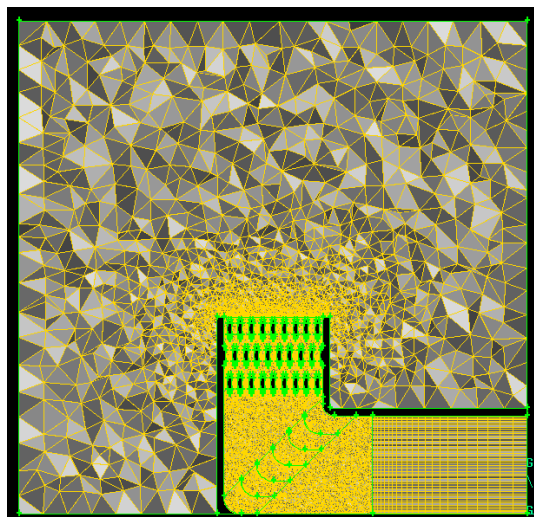


Figure 8: Effect of cross-wind simulation CFD mesh
 6 different scenarios including five wind directions and one no wind condition were solved and are as follows:

- No Wind
- +Z
- -Z
- -X
- +Z-X
- -Z-X

The wind profile was of the power law type [Equation 1] as described in CFD simulations of the wind Environment around an Airport Terminal Building [viii] and is applied to the appropriate boundaries in the model.

$$\left(U = U_{ref} \left(\frac{z}{z_{ref}} \right)^a \right)$$

Equation 1

This profile is validated with experimental data at an airport of comparable layout. The profile was implemented using a UDF in Fluent; which was applied to the upwind velocity inlet boundary. In the case of diagonal winds, the UDF was rewritten using Pythagora's theorem and applied to the two upwind boundaries. The profile has a reference velocity of 10ms^{-1} at a reference height of 14m (the height of the test cell inlet).

Contour plots of velocity at a plane in the XY direction for each of the wind cases is shown below.

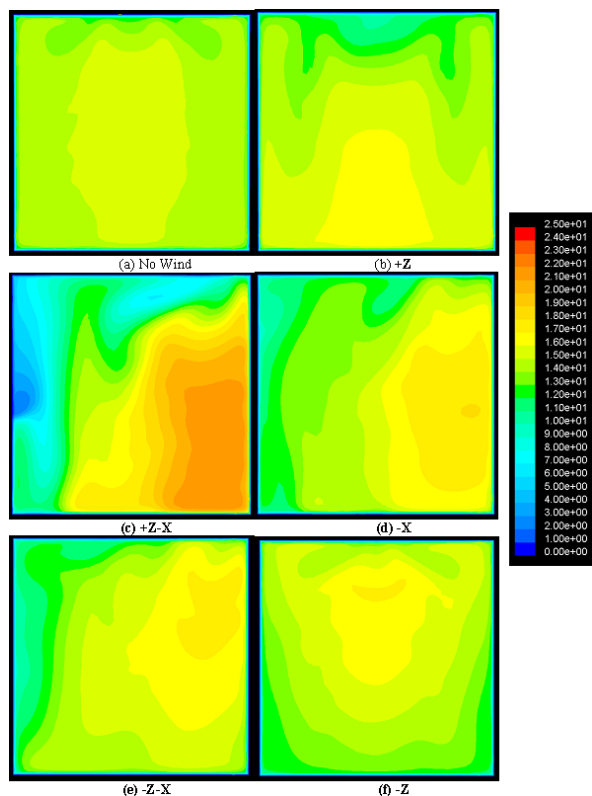


Figure 9: XY plane velocity contour plots for each cross wind case

VI. DISCUSSION

Figure 5 shows that the no vortex condition requires a cell bypass ratio of more than 50-70% (the value varying with H/D_i), justifying the rule of thumb used in test cell design that a cell bypass ratio of more than 80% must be used to prevent vortex formation. Below the no-vortex region, there is a wide band of CBR at which an unsteady, unstable vortex is seen, equivalent to the unsteady, inconstant vortices observed in some real test cells. At CBRs of less than 20-30% a stable vortex is seen in the calculations.

The threshold for vortex formation predicted shows the following trends

1. Vortices form when the upstream velocity is low and are blown downstream and vanish as upstream velocity increases above the “blow away” velocity.
2. On a V_i/V_o against H/D_i plot (Figure 6) the threshold for vortex formation shows a positive gradient i.e. as the height of the suction inlet increases, the blow-away velocity decreases.
3. As the upstream average gradient increases, the range of conditions in which a vortex is formed (steady or deformed vortex) increases.

All the trends agrees with previous experimental data by various authors (Nakayama and Jones [ix], Liu et al. [x] and Shin et al. [xi]) and is similar to numerical data by Jermy and Ho [iv] on a suction inlet over ground plane model.

Figure 9 shows that wind blowing around the intake stack of U-shaped test cell has significant effects on the upstream velocity profile. An upstream velocity gradient in the direction perpendicular to the suction tube can be generated when some component of wind blowing is in the same direction (i.e. wind with a +X component will generate a velocity gradient in the +X direction and vice versa). This gradient maybe the origin of the vorticity required to form the

vortex. However anecdotal evidence have been observed in still conditions so it is unlikely that this is the sole source of vorticity.

VII. CONCLUSIONS

The scenario of a suction inlet in a box, resembling a test cell configuration, has been studied and the threshold for vortex formation extracted.

Three cases of vortex formation are observed as mentioned by Ho and Jermy [i]: no vortex, an unsteady, unstable deformed vortex, and a stable regular vortex.

In agreement with previous studies, the vortex threshold has a positive gradient when plotted on a V_i/V_o against H/D_i graph. As the upstream average gradient increases, the range of conditions in which a vortex is formed (steady or deformed vortex) increases.

The threshold cell bypass ratio is relatively constant with H/D_i . No vortex is formed with cell bypass ratios greater than 50-70%, and stable vortices are formed at cell bypass ratios less than 20-30%. The exact value of the cell bypass ratio threshold varies with H/D_i .

Wind blowing around the intake stack of a U-shaped test cell has significant impact on the generation of upstream velocity gradient.

Further investigation on the effects of the other parameters mentioned above has on the threshold, as detailed above, will be carried out.

ACKNOWLEDGEMENT

We would like to thank CENCO Inc., SAFRAN Group for financial support and technical discussions and in particular Rich Kruse.

REFERENCES

- [i] Ho W.H., Jermy M., “Validated CFD simulations of vortex formation in jet engine test cells”. 16th Australasian Fluid Mechanics Conference Proceedings Pg 1102 – 1107 (2007)
- [ii] Karlsson A. Fuchs L., “Time evolution of the vortex between an air inlet and the ground”, AIAA paper 2000-0990 (2000)
- [iii] Secareanu A., Morioanu D., Karlsson A. and Fuchs L., “Experimental and numerical study of ground vortex interaction in an air-intake”, AIAA paper 2005-1206 (2005)
- [iv] Jermy M., Ho W.H., “Location of the vortex formation threshold at suction inlets near ground planes by CFD simulation”, Proc. IMechE Part G J.Aero.Eng., Accepted for publication 21st Jan 2008
- [v] Glenn D. E., “Ingestion of debris into intakes by vortex action”, Aeronautical Research Council CP No 1114 (1970)
- [vi] Kline H., “Small scale tests on jet engine pebble aspiration tests”, Douglas Aircraft Company, Report SM-14885 (1953)
- [vii] Ridder S.O., Samuelsson I., “An experimental study of strength and existence of domain of ground-to-air inlet vortices by ground board static pressure measurements”, Stockholm Royal Institute of Technology, KTH AERO TN 62

[viii] Neofytout P., Venestsanos A. G. et al., “CFD Simulations of the Wind Environment around an Airport Terminal Building” QNET CFD Newsletter, July 2003

[ix] Nakayama A., Jones J.R., “Vortex formation in inlet flow near a wall”, 24th Aerospace and Sciences Meeting and Exhibit, AIAA 96-0803 (1996)

[x] Liu W., Greitzer E.M. and Tan C.S., “Surface static pressure in an inlet vortex flow field”, ASME Journal of Engineering for Gas Turbines and Power, 107, pp 387—393 (1985)

[xi] Shin H.W., Cheng W.K., Greitzer E.M., Tan C.S., and Shippee C.L., “Circulation measurements and vortical structure in an inlet-vortex flow field”, J. Fluid Mech. 162 pp 463-487 (1986)